Desalination and Water Treatment
www.deswater.com
doi: 10.1080/19443994.2016.1193770

57 (2016) 28646–28660
December

Taylor & Francis
Taylor & Francis Group

Neural network approach for predicting solar still production using agricultural drainage as a feedwater source

Ahmed F. Mashaly[a,*], A.A. Alazba[a,b]

[a]*Alamoudi Chair for Water Researches, King Saud University, Riyadh, Saudi Arabia, Tel. +966 14673737; Fax: +966 14673739; emails: amashaly@ksu.edu.sa, mashaly.ahmed@gmail.com (A.F. Mashaly), alazba@ksu.edu.sa (A.A. Alazba)*
[b]*Agricultural Engineering Department, King Saud University, Riyadh, Saudi Arabia*

Received 27 January 2016; Accepted 20 May 2016

ABSTRACT

This study investigates the application of artificial neural network (ANN) for predicting solar still production (MD). Agricultural drainage water (ADW) was desalinated using a solar still. Important meteorological variables: ambient air temperature, relative humidity, wind speed, and solar radiation, together with the operational variables of flow rate, temperature, and total dissolved solids of feedwater, were considered as input parameters for ANN modeling. The output parameter was MD. The results revealed that the ANN model with five neurons and hyperbolic tangent transfer function was the most appropriate for MD prediction based on the minimum measures of error. The optimal ANN model had a 7–5–1 architecture. The ANN model was also compared to multiple linear regression (MLR). The results indicated that, compared to the MLR model, the ANN model provided better prediction results in all modeling stages. The average of the coefficient of determination between the ANN results and the experimental data was more than 0.96. Consequently, the ANN model was shown to have acceptable generalization capability and accuracy. The relative errors of forecasted MD values for the ANN model were mostly in the vicinity of ±10%. These results indicate that ANN can be successfully used in the MD prediction of a solar still desalinating ADW. One major output/contribution of this research involves assessment of the ANN modeling technique during ADW solar desalination, which adds a new perspective to the system analysis, design, and modeling for the potential productivity of a solar still to produce water during the ADW desalination process.

Keywords: Agricultural drainage water; Artificial neural network; Solar still; Desalination; Modeling

1. Introduction

Water scarcity raises the need to explore all possible options to maintain the current water resources and explore new alternative sources. The availability of ample quantities of agricultural drainage water (ADW) creates considerable opportunities for recovering significant quantities of water from this water source [1]. Globally, nearly two-thirds of the water delivered to irrigated crops is lost as ADW or run-off, or both [2]. In recent years, there has been an interest in using desalination as a potentially viable method for the reclamation of ADW for irrigation and possibly potable water consumption [3], and this helps in the

*Corresponding author.

face of growing demand for water. One of the interests for using desalinated water in the irrigation and agricultural sector, in general, is that the use of desalinated water increases the yield [4] and quality of some agricultural products and at the same time results in lower water consumption and recovery of salinity-affected soils [5].

The sun as an energy source for the desalination process using solar stills can potentially offer a viable way to treat and desalinate ADW, producing economically valuable high-quality water for either irrigation or even drinking. Solar stills are the most attractive and simplest method among other solar desalination methods for ADW. A solar still uses a sustainable and pollution-free source to yield high-quality water. The major problem of the solar still is its low productivity. The most important thing in attempts to increase still productivity is to maintain economic feasibility and simplicity [6]. Adhikari et al. [7] stated that the productivity of a solar still is always a prime design target.

Based on the foregoing, solar stills required for ADW desalination must be carefully selected based on the productivity of these stills. This is very difficult owing to numerous measurement and heat transfer computations. Consequently, construction of mathematical models for the prediction of solar still productivity is a useful mean and valuable tool. These models play an important role in the simulation and optimization of solar still productivity leading to efficient and economical designs. And by knowing and forecasting the productivity, it would be easy to develop plans to exploit this new non-conventional source of water in the agricultural sector after the solar desalination process, either directly or indirectly through mixing with water of low quality to increase the volume of water available for the agricultural sector.

On the other hand, the mathematical algorithms used for these computations are still complicated, involving the solution of complex equations and requiring large computational power and need a considerable long computational time [8]. With the progress in computer technology and mathematical modeling techniques, the employment and usage of Artificial Neural Networks (ANNs) in solar desalination by stills could achieve results that are not facilely obtained with classical modeling techniques.

ANNs are biologically inspired computer systems designed to mimic the method in which the human brain processes information. Interrelationships of correlated parameters that symbolically denote the interconnected processing neurons/nodes of the human brain are used to develop models. Pachepsky et al. [9] stated that ANNs find relationships by observing several input and output examples to develop a formula that can be used for predictions. Non-linear relationships overlooked by other techniques can be set with little a priori knowledge of the functional relationship [10]. There has been a growing trend for ANNs for modeling and simulation in the areas of agricultural, environmental, and energy engineering. Some examples are:

Safa and Samarasinghe [11] used ANN technique for estimation and modeling of energy consumption in wheat production. Gocic´ et al. [12] computed reference evapotranspiration by ANN. Yang et al. [13] developed an ANN model to emulate DRAINMOD. KAshefipour et al. [14] modeled drainage water salinity for agricultural lands using ANN. Schaap and Bouten [15] simulated soil–water retention curves using ANN. In the solar field, Lecoeuche and Lalot [16] applied ANN to forecast the *in situ* daily performance of solar air collectors. Farkas and Geczy-Víg [17] developed ANN models for different solar collectors to forecast the outlet temperature. Sözen et al. [18] the ANN technique was applied to calculate the efficiency of solar collectors. ANNs have been used to model and forecast various solar still performances ranging from determining the effectiveness of modeling distillate yield using local weather data [19] and using different learning algorithms [20], to assess and optimize solar still performance under hyperarid environment [21], or instantaneous thermal efficiency prediction [22].

However, the optimal performance of solar desalination of ADW is closely related to the successful selection and operation of a solar still whose selection is the backbone of the entire process. Accordingly, solar stills should be optimally designed and operated, and prediction of its productivity is one of the essential parameters to be accurately determined. Forecasting of still productivity helps to know the potential productivities attainable by the still and to ensure the adequacy of distillation/desalination to produce water that can be used for various agricultural purposes. There is a need to develop a predictive model that would be able to accurately determine still productivity. The aims of this study are to (1) develop predictive mathematical model to calculate the solar still productivity using ANNs; (2) assess the performance of the developed ANN model using a statistical comparison between the results of solar still productivity obtained from the developed ANN model and experimental findings; and (3) compare the developed ANN model with multiple linear regression (MLR) model in terms of their appropriateness for forecasting solar still productivity during ADW desalination.

2. Materials and methods

2.1. Experimental setup

The experiments were conducted at the Agricultural Research and Experiment Station at the Department of Agricultural Engineering, King Saud University, Riyadh, Saudi Arabia (24°44′10.90′′N, 46°37′13.77′′E) between October and November 2013. The weather data were obtained from a weather station (model: Vantage Pro2; manufacturer: Davis, USA) close by the experimental site (24°44′12.15′′N, 46°37′14.97′′E). The solar still system used in the experiments was constructed from a 6 m^2 single-stage C6000 panel (F Cubed. Ltd, Carocell Solar Panel, Australia). The solar still panel was manufactured using modern, cost-effective materials such as coated polycarbonate plastic. When heated, the panel distilled a film of water that flowed over the absorber mat of the panel. The panel was fixed at angle of 29° from the horizontal plane. The basic construction materials were galvanized steel legs, an aluminum frame, and polycarbonate covers. The transparent polycarbonate was coated on the inside with a special material to prevent fogging (patented by F Cubed, Australia). Cross-sectional view of the solar still is presented in Fig. 1. The work idea of the system is summarized in these paragraphs.

The water was fed to the panel using centrifugal pump (model: PKm 60, 0.5 HP, Pedrollo, Italy) with a constant flow rate was 10.74 L/h. The feed was supplied by eight drippers/nozzles, creating a film of water that flowed over the absorbent mat. Underneath the absorbent mat was an aluminum screen that helps to distribute the water across the mat. Beneath the aluminum screen was aluminum. Aluminum was chosen for its hydrophilic properties, to assist in the even distribution of the sprayed water. Water flows through and over the absorbent mat, and solar energy was absorbed and partially collected inside the panel; as a result, the water is heated and hot air is circulated naturally within the panel. First, the hot air flowed toward the top of the panel, and then reversed its direction to approach the bottom of the panel. During this process of circulation, the humid air touches the cooled surfaces of the transparent polycarbonate cover and the bottom polycarbonate layer, causing condensation. The condensed water flowed down the panel and was collected in the form of a distilled stream. Agricultural drainage water (ADW) was used as a feedwater input to the system. The solar still system was run from 10 May 2013 to 11 January 2013. Raw ADW was obtained from Al-Oyun City, Al-Ahsa, in Eastern Saudi Arabia (25°35′7.02′′N, 49°35′48.17′′E). The initial concentration of total dissolved solids

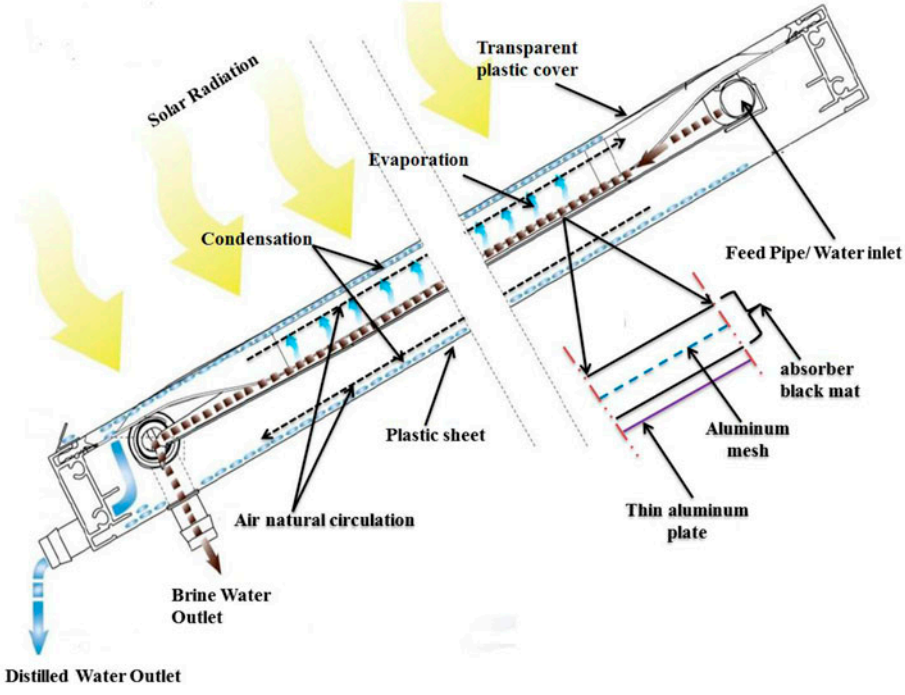

Fig. 1. Cross-sectional view of the solar still.

(TDS) in the ADW, along with their pH, density (ρ) and electrical conductivity (EC), are listed in Table 1. The productivity or the amount of distilled water produced (MD) during a time period by the system was obtained by collecting the cumulative amount of water produced over time. The temperature of the feedwater (T_F) was measured using thermocouples (T-type, UK). Temperature data for feed brine water were recorded on a data logger (model: 177-T4, Testo, Inc., UK) at 1 min intervals. The amount of feedwater (M_F) was measured by calibrated digital flow meter was mounted on the feedwater line (micro-flo, Blue-White, USA). The amount of brine water and distilled water were measured by graduated cylinder. TDS concentration and EC were measured using a TDS-calibrated meter (Cole-Parmer Instrument Co. Ltd., Vernon Hills, USA). A pH meter (model: 3510 pH meter, Jenway, UK) was used to measure pH. A digital-density meter (model: DMA 35_N, Anton Paar, USA) was used to measure ρ. The ADW was fed separately to the panel using the pump described above. The residence time —the time taken for the water to pass through the panel—was approximately 20 min. Therefore, the flow rate of the feedwater, the distilled water, and the brine water was measured each 20 min. Also, the total dissolved solids of feedwater (TDS_F) were measured every 20 min. The weather data such as air temperature (T_o), relative humidity (RH), wind speed (WS), and solar radiation (SR) were obtained from the weather station mentioned above. Here, there is one dependent variable which was the MD of solar desalination/still system and seven independent variables which are T_o, RH, WS, SR, TDS_F, M_F, and T_F.

2.2. Artificial neural networks (ANNs)

An ANN is analogous to a biological nervous system and comprises an input layer, a hidden layer(s), and an output layer [23]. A certain number of small individual and interconnected processing elements named neurons or nodes are present in each layer. The nodes are connected to each other by communication links associated with connection weights, and signals are passed through nodes the over the connection weights. Each node receives multiple inputs from other nodes in proportion to their connection weights and creates a single output signal that may be propagated to other nodes [24–26]. According to Demuth and Beale [27], each artificial neuron is a unitary computational processor with a summing junction operator and a transfer/activation function. The connections between inputs, neurons, and outputs comprise weights (W) and biases (B). The most widely used ANN type for modeling and forecasting is Multi-Layer Perception (MLP) [28,29]. The mathematical expression of the ANN model can be written as:

$$Y = F\left(\sum_{j=1}^{m} W_{kj} F\left(\sum_{i=1}^{n} W_{ji} X_i + B_j\right) + B_k\right) \quad (1)$$

where Y is the output (MD), W_{kj} are the weights between hidden and output layers, W_{ji} are the weights between input and hidden layers, X_i are input variables (T_o, RH, WS, SR, TDS_F, M_F, and T_F), m is the number of neurons in the hidden layer, n is the number of neurons in the input layer, B_j and B_K are the bias values of the neurons in the hidden layer and output layer, respectively, and F is the transfer function. The transfer/activation functions used in the present study were sigmoid and hyperbolic tangent transfer functions: the sigmoid transfer function (SIG) for any variable V was:

$$F(V) = \frac{1}{1 + \exp(-V)} \quad (2)$$

and the hyperbolic tangent transfer function (TANH) for any variable V was:

$$F(V) = \frac{1 - \exp(-2V)}{1 + \exp(-2V)} \quad (3)$$

ANN model development involves the use of experimental data for model training, evaluation, and testing of different ANN configurations. This ultimately leads to the selection of an optimum configuration and ideally validation with a new data-set not used in training. A flowchart describing the developing procedure of the ANN is shown on Fig. 2. Qnet2000 software was used to develop the ANN model using, in training process, the most prevalent learning algorithm called the back-propagation (BP) algorithm [30]. In order to develop an ANN model, the network is processed through three phases: training/learning stage,

Table 1
Some properties of the agricultural drainage water used for desalination process

Property	Agricultural drainage water
TDS (PPT)	4.71
pH	8.1
ρ (g/cm^3)	1.001
Ec (mS/cm)	7.54

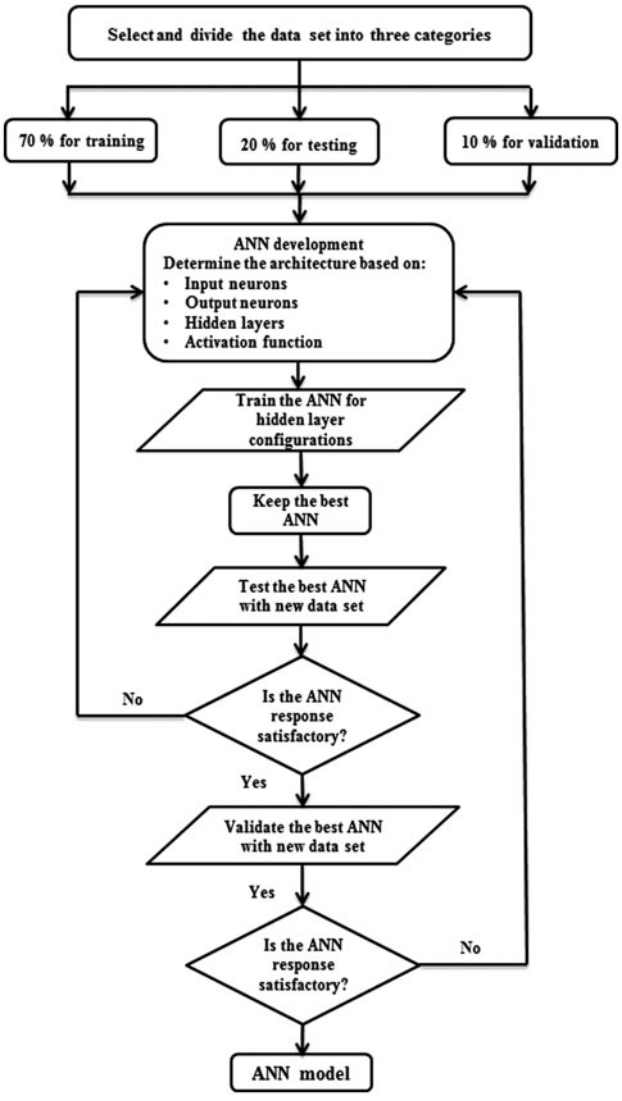

Fig. 2. Flow chart for developing ANN model.

testing stage, and validation stage. In the training phase, the ANN is trained to forecast an output. In the testing phase, the ANN is tested to stop training or to keep in training and it is used to predict an output. In the validation phase, the ANN is validated to check the performance on new cases. The data-set, which comprised 56 data points obtained from the experimental work, was divided randomly into training (70%), testing (20%), and validation (10%) subsets. Therefore, the training, testing, and validation sets have 39, 11, and 6 data points, respectively. Kalogirou et al. [24] used 54 data points for developing an ANN model which successfully and accurately predicted the performance of a solar water heater.

The best method to find the optimal number of neurons in hidden layer is using trial-and-error procedure [31]. Trial-and-error method was used to determine the optimum neurons in hidden layer of the network. Before modeling process, the data are automatically normalized between 0.15 and 0.85. The normalization process accelerates the training and increases the network's generalization capabilities. The iteration was fixed to 10,000. The learning rate and momentum factor were fixed and were to be 0.01 and 0.8, respectively.

$$X_n = \left(\frac{X_o - X_{\min}}{X_{\max} - X_{\min}}\right) \times (0.85 - 0.15) + 0.15 \quad (4)$$

where X_o is the original values of input and output variables, X_n is normalized value and $X_{\max}$ and $X_{\min}$ are maximum and minimum values of input and output variables, Table 2.

2.3. Multiple linear regression analysis (MLR)

MLR is a statistical technique used to model the linear relationship between a dependent parameter and one or more independent parameters. MLR method is based on least squares, so the model is fit such that the sum of squares of differences of observed and predicted values are diminished. An MLR has been conducted for the prediction of MD. MLR model was carried out using IPM SPSS statistics 22. A general MLR model can be written as [32]:

$$Y = \beta_0 + \beta_1 X_1 + \beta_2 X_2 + \cdots + \beta_R X_R \quad (5)$$

where Y is the predicted parameter, X_i (i = 1, 2, … , R) are the predictors, β_0 is the intercept, β_i (i = 1, 2, …, R) is the coefficient on the ith predictor. The MLR model was developed based on the same input-independent parameters and output-dependent parameter as used in the developed ANN model.

2.4. Criteria of evaluation

The performance of the ANN and MLR models was assessed with statistical and graphical comparisons. To assess the accuracy of the prediction models, the coefficient of determination (R^2), the root mean square error (RMSE), the mean absolute error (MAE), the coefficient of model efficiency (ME), the overall index of model performance (OI), and the coefficient of residual mass (CRM) were used. The R^2, RMSE,

Table 2
Statistical analysis of input and output parameters

Variable	Unit	AVG	MIN	MAX	SD	KU	SK	CV
T_o	℃	32.95	24.30	39.36	4.28	−0.96	0.07	0.13
RH	%	13.88	7.81	30.19	6.16	0.35	1.14	0.44
WS	km/h	1.39	0.00	5.18	1.56	−0.16	1.09	1.12
SR	W/m^2	665.42	223.19	810.05	137.85	1.38	−1.29	0.21
T_F	℃	37.99	29.39	42.75	2.81	0.58	−0.13	0.07
M_F	L/min	0.17	0.16	0.18	0.00	0.68	−1.40	0.03
TDS_F	PPT	28.14	4.71	99.43	25.69	0.87	1.36	0.91
MD	L/m^2/h	0.60	0.16	0.91	0.18	−0.28	−0.59	0.30

Notes: AVG: average value, MIN: minimum value, MAX: maximum value, SD: standard deviation, KU: Kurtosis, SK: Skewness, CV: coefficient of variation.

MAE, ME, OI, and CRM values (were calculated using Eqs. (6)–(11), respectively [33–35]:

$$R^2 = \frac{\left(\sum_{i=1}^{n}\left(x_{o,i}-\overline{x}_o\right)\left(x_{p,i}-\overline{x}_p\right)\right)^2}{\sum_{i=1}^{n}\left(x_{o,i}-\overline{x}_o\right)^2 \times \sum_{i=1}^{n}\left(x_{p,i}-\overline{x}_p\right)^2} \tag{6}$$

$$\mathrm{RMSE} = \sqrt{\frac{\sum_{i=1}^{n}\left(x_{o,i}-x_{p,i}\right)^2}{n}} \tag{7}$$

$$\mathrm{MAE} = \frac{\sum_{i=1}^{n}\left|x_{o,i}-x_{p,i}\right|}{n} \tag{8}$$

$$\mathrm{OI} = \frac{1}{2}\left(1-\left(\frac{\mathrm{RMSE}}{x_{\max}-x_{\min}}\right)+\mathrm{ME}\right) \tag{9}$$

$$\mathrm{ME} = 1-\frac{\sum_{i=1}^{n}\left(x_{o,i}-x_{p,i}\right)^2}{\sum_{i=1}^{n}\left(x_{o,i}-\bar{x}_o\right)^2} \tag{10}$$

$$\mathrm{CRM} = \frac{\left(\sum_{i=1}^{n}x_{p,i}-\sum_{i=1}^{n}x_{o,i}\right)}{\sum_{i=1}^{n}x_{o,i}} \tag{11}$$

where $x_{o,i}$ is the observed value; $x_{p,i}$ is the predicted value; $x_{\min}$ is the minimum observed value; $x_{\max}$ is the maximum observed value; $\bar{x}_o$ is the averaged observed values; $\bar{x}_p$ is the averaged predicted values; and n is the number of observations.

The higher R^2 values show the greater similarities between observed and predicted values. The RMSE and MAE values can range from 0 to ∞. The lower RMSE and MAE values demonstrate the more accurate prediction results. An ME value of 1.0 means a perfect fit between observed and forecasted results. ME value can be negative. An OI value of 1 represents an ideal fit between the observed and forecasted data [35]. The CRM values are in the vicinity of ±1. The closer CRM is to zero, the better the model accuracy. For ideal data modeling, RMSE, MAE, CRM should be closer to zero, but values of R^2, ME, and OI should approach to 1 as closely as possible.

3. Results and discussion

3.1. Data processing and general performance

Statistical analyses and data processing were performed using the data analysis tool in Microsoft Excel. Table 2 shows the statistical summary of experimental data and the parameters used for training, testing, and validation of the model. The minimum (MIN), maximum (MAX), mean (AVG), standard deviation (SD), Skewness (SK), Kurtosis (KU), and coefficient of variation (CV) are shown in Table 2. As Table 2 also shows, for the independent variables T_o, RH, WS, SR, T_F, M_F, and TDS_F, variations were 24.30–39.36℃, 7.81–30.19%, 0.00–5.18 km/h, 223.19–810.05 W/m^2, 29.39–42.75℃, 0.16–0.18 L/min, and 4.71–99.43 PPT, respectively. With a mean of 28.14 PPT, the value of available TDS_F is not valid for either drinking or any other use (e.g. irrigation). After desalination, fresh water produced showed a TDS of 0.100 PPT [36], which not only falls within the acceptable range according to WHO [37], but is also considered excellent, and moreover appropriate for application in greenhouses' cultivation in both irrigation and cooling systems. The dependent variable, MD, varied from 0.16 to 0.91 L/m^2/h, with an average value of 0.60 L/m^2/h. The distribution curves for all independent and dependent variables are platykurtic because KU values did not exceed 3. Distribution was highly skewed for RH, WS, SR, M_F, and TDS_F, moderately skewed for MD, and approximately symmetric for T_o and T_F. As CV values make clear, data for T_F and M_F were homogenous. T_o was relatively homogeneous and SR was relatively heterogeneous. The data for RH, WS, TDS_F, and MD were heterogeneous.

A correlation matrix of all input and output variables is displayed in Table 3. This table shows that the

linear correlation between SR and MD is 0.89. The results indicate that the SR has the most significant correlation. Hence, any model that uses SR should be able to estimate the MD satisfactorily. The accuracy of the model can be enhanced by considering other variables with impacts on MD. The T_o, RH, WS, T_F, M_F, and TDS_F are not well-correlated with MD. These variables are included in our model for better accuracy of MD estimation. All these correlations between variables and MD are positive, except WS and M_F, which are negative. According to the results of the field experiments, the average MD for the solar still system was 0.60 L/m^2/h (approximately 5 L/m^2/d). This is consistent with the results of [38–41]. It is observed that the MD of the still increased as the SR increases until it achieves their maximum value around noon and then decrease with the decrease in SR. This is due to evaporation rate, which primarily depends on the SR, and this is in agreement with [42]. A more complete demonstration of these experimental data is given by [36]. Also, a detailed discussion and analysis of comparative investigation between MD and crop water requirement to determine the required area of the solar still system can be found in [43].

3.2. Selection of optimum ANN architecture

Table 4 shows the results of the statistical performance of the ANN model with different node numbers in the hidden layer and different transfer/activation functions. The best ANN architecture was selected through a trial-and-error method based on the statistical measures displayed in Table 4. This means that trial-and-error method was used to determine the optimum neurons/nodes in hidden layer of the ANN model (examined from 2 to 10 neurons). Transfer function was varied between SIG and TANH in the hidden layer. To optimize the ANN architecture, the trials started using 2 nodes in the hidden layer as the initial guess. As shown in the first row in Table 4, the values of standard deviation (SD), maximum error (MXE), and correlation coefficient (CC) were 0.037, 0.085, and 0.978 L/m^2/h, respectively. Furthermore, R^2, RMSE, ME, OI, CRM, and MAE values were 0.956, 0.037 L/m^2/h, 0.956, 0.954, −0.002, and 0.029 L/m^2/h, respectively. The ANN performance has been improved for the same construction (7–2–1) using TANH function, where SD, CC, and MXE were 0.021, 0.055, and 0.993 L/m^2/h, respectively. Furthermore, the statistical parameter values of R^2, RMSE, ME, OI, CRM, and MAE are 0.986, 0.021 L/m^2/h, 0.986, 0.979, −0.001, and 0.017 L/m^2/h. The 7–3–1 and 7–4–1 architectures of the ANN model gave a slight improvement reflected in the values of the statistical measures as seen in the Table 4. Increasing the neuron number to five (7–5–1) gave a clear and a marked improvement in the ANN model performance, particularly for the TANH function. This function gave the best network performance, where the SD, CC, and MXE values were 0.018, 0.041, and 0.995 L/m^2/h, respectively. Also, the values of R^2, RMSE, ME, OI, CRM, and MAE are 0.990, 0.018 L/m^2/h, 0.990, 0.983, −0.001, and 0.015 L/m^2/h. Increasing the number of hidden neurons above 5 affects adversely somewhat on the ANN model. Based on the foregoing, there was an obvious improvement in the developed ANN model when the number of hidden neurons was increased to 5 and the TANH function was used. As seen from the results in Table 4, the TANH function was better than SIG function during all trials in the prediction of MD. As a result, the most appropriate ANN architecture is 7–5–1 with the TANH function (bolded in Table 4), as this gave the best MD prediction with the lowest error (the minimum RMSE, CRM, and MAE; and the maximum R^2, ME, and OI). The best architecture of the developed ANN model is schematically illustrated in Fig. 3.

The average contribution to the optimum ANN architecture of each input node (variable) on the output is

Table 3
Correlation matrix between input and output variables

	T_o	RH	WS	SR	T_F	M_F	TDS_F	MD
T_o	1.00							
RH	−0.48	1.00						
WS	−0.68	0.03	1.00					
SR	−0.28	0.05	0.19	1.00				
T_F	0.93	−0.49	−0.47	−0.20	1.00			
M_F	0.00	−0.72	0.42	0.05	0.08	1.00		
TDS_F	−0.33	0.72	−0.15	−0.07	−0.41	−0.84	1.00	
MD	0.02	0.11	−0.11	0.89	0.07	−0.22	0.07	1.00

Notes: T_o: ambient temperature, RH: relative humidity, WS: wind speed, SR: solar radiation, T_F: feed temperature, M_F: feed flow rate, TDS_F: total dissolved solids of feed, MD: solar still water productivity.

Table 4
Statistical performance of the ANN model with various node numbers in the hidden layer and transfer functions (the bold refers to the optimum architecture)

		Network statistics				Statistics parameters					Average contribution of input node on output (%)						
ANN	TF	SD	MXE	CC	R^2	RMSE	ME	OI	CRM	MAE	T_o	RH	WS	SR	T_F	M_F	TDS_F
7–2–1	SIG	0.037	0.085	0.978	0.956	0.037	0.956	0.954	−0.002	0.029	15.58	7.84	3.91	59.96	2.90	5.56	4.25
	TANH	0.021	0.055	0.993	0.986	0.021	0.986	0.979	−0.001	0.017	22.07	10.65	1.14	47.62	10.19	2.85	5.49
7–3–1	SIG	0.039	0.093	0.975	0.950	0.039	0.950	0.949	−0.001	0.030	14.40	6.74	4.17	61.75	0.99	6.50	5.46
	TANH	0.021	0.053	0.993	0.986	0.021	0.986	0.979	0.000	0.017	23.89	14.27	0.48	41.99	9.85	4.63	4.89
7–4–1	SIG	0.039	0.089	0.976	0.952	0.039	0.952	0.950	−0.002	0.030	16.49	7.63	3.29	59.15	3.81	5.24	4.41
	TANH	0.023	0.068	0.992	0.984	0.023	0.984	0.977	0.000	0.017	22.94	15.24	0.93	44.23	9.90	4.03	2.73
7–5–1	SIG	0.038	0.086	0.977	0.954	0.038	0.954	0.952	−0.002	0.029	15.87	7.50	3.63	59.92	3.06	5.61	4.42
	TANH	**0.018**	**0.041**	**0.995**	**0.990**	**0.018**	**0.990**	**0.983**	**−0.001**	**0.015**	**21.53**	**11.37**	**2.56**	**44.40**	**9.80**	**3.87**	**6.46**
7–6–1	SIG	0.038	0.091	0.976	0.953	0.038	0.952	0.951	−0.003	0.031	14.33	8.40	4.57	62.96	0.42	4.94	4.38
	TANH	0.019	0.042	0.994	0.988	0.019	0.988	0.982	−0.001	0.016	23.66	11.79	1.27	43.08	11.01	4.37	4.83
7–7–1	SIG	0.038	0.093	0.976	0.952	0.038	0.952	0.950	−0.002	0.030	14.61	8.04	4.23	62.79	0.22	4.83	5.27
	TANH	0.021	0.045	0.993	0.986	0.021	0.986	0.979	−0.001	0.017	22.94	12.36	3.43	42.24	10.41	3.91	4.70
7–8–1	SIG	0.038	0.088	0.976	0.953	0.038	0.953	0.951	−0.003	0.031	15.80	9.20	4.05	61.22	1.58	3.71	4.44
	TANH	0.019	0.054	0.994	0.988	0.019	0.988	0.981	−0.001	0.015	21.40	10.10	3.07	45.05	12.10	2.85	5.43
7–9–1	SIG	0.039	0.089	0.975	0.951	0.039	0.951	0.949	−0.003	0.031	16.54	8.56	3.35	60.24	2.26	3.97	5.07
	TANH	0.020	0.049	0.993	0.987	0.020	0.987	0.980	0.000	0.016	23.38	14.76	1.55	42.76	10.02	4.71	2.82
7–10–1	SIG	0.038	0.090	0.976	0.952	0.038	0.952	0.951	−0.003	0.031	15.24	9.06	4.14	62.43	0.30	3.60	5.22
	TANH	0.018	0.040	0.995	0.989	0.018	0.989	0.982	−0.001	0.015	21.96	11.33	2.93	44.26	10.79	3.41	5.30

Notes: TF: transfer function, SD: standard deviation, MXE: maximum error, CC: correlation coefficient, R^2: coefficient of determination, RMSE: root mean square error, ME: model efficiency, OI: overall index of model performance, CRM: coefficient of residual mass, MAE: mean absolute error.

presented in Table 4 (in bold). These values illustrate the relative importance of each input parameter to the training of the developed ANN model and are commonly used to select the input variables in problems with many inputs. Additionally, this contribution analysis can indicate which variables are the most significant (with the highest contribution values) in comparison with other inputs. Based on these analyses, the variables with the smallest contribution are WS (2.56%) and M_F (3.87%), while RH, T_F and TDS_F have moderate effects on the predicted MD with contributions percentage of 11.37, 9.80, and 6.46%, respectively. The variables with the highest contributions are SR (44.4%) and T_o (21.53%); it is clear that these are the most significant parameters that affect MD due to their role in radiant and convective transfer of energy into the solar still system and their function as sources of energy. These results are in agreement with previous studies [44,45], which reported that MD was significantly affected by SR and T_o. The developed ANN model can be easily programmed and solved in a spreadsheet (i.e. Microsoft Excel) or in the programming language Visual Basic. The ANN model can be formulated by an algebraic system of equations as follows:

3.3. ANN performance analysis and comparison with MLR

The statistical performance of the developed ANN model is given in Table 6. This table indicates that the ANN model performed excellently, predicting results with very low error The level of error present in this model is acceptable when predicting MD values. In order to highlight the accuracy and necessity of using the developed ANN, the results must also be obtained using an MLR model. The MLR model was created to confirm the efficiency of the developed ANN model. The MLR model was also applied to the same inputs and output parameters which used for the ANN model. The MLR model can be written as follows:

$$\mathrm{MD} = -0.404 + 0.028T_o + 0.007\mathrm{RH} + 0.003\mathrm{WS} + 0.001\mathrm{SR} - 0.019T_F - 1.036M_F + 0.001\mathrm{TDS}_F \quad (18)$$

The SE of regression coefficients, *t*-stat and *p*-value of independent variables (T_o, RH, WS, SR, T_F, M_F and TDS_F) are displayed in Table 5. The MLR model showed that all independent variables were directly proportional to MD, except T_F and M_F which were inversely proportional to MD. The *SE* measures the accuracy of the

$$\mathrm{MD} = \frac{1 - \exp[(-3.83 \times F_1 + 0.31 \times F_2 + 4.31 \times F_3 - 2.05 \times F_4 - 1.06 \times F_5) + 0.54]}{1 + \exp[(-3.83 \times F_1 + 0.31 \times F_2 + 4.31 \times F_3 - 2.05 \times F_4 - 1.06 \times F_5) + 0.54]} \quad (12)$$

where F_1, F_2, F_3, F_4, and F_5 are calculated as follows:

$$F_1 = \frac{1 - \exp[(-1.85 \times T_o + 1.71 \times \mathrm{RH} + 0.75 \times \mathrm{WS} - 1.74 \times \mathrm{SR} + 0.26 \times T_F - 0.68 \times M_F + 1.84 \times \mathrm{TDS}_F) + 2.59]}{1 + \exp[(-1.85 \times T_o + 1.71 \times \mathrm{RH} + 0.75 \times \mathrm{WS} - 1.74 \times \mathrm{SR} + 0.26 \times T_F - 0.68 \times M_F + 1.84 \times TDS_F) + 2.59]} \quad (13)$$

$$F_2 = \frac{1 - \exp[(0.17 \times T_o - 0.56 \times \mathrm{RH} + 0.72 \times \mathrm{WS} - 0.45 \times \mathrm{SR} - 0.33 \times T_F + 0.25 \times M_F + 0.40 \times \mathrm{TDS}_F) - 0.46]}{1 + \exp[(0.17 \times T_o - 0.56 \times \mathrm{RH} + 0.72 \times \mathrm{WS} - 0.45 \times \mathrm{SR} - 0.33 \times T_F + 0.25 \times M_F + 0.40 \times \mathrm{TDS}_F) - 0.46]} \quad (14)$$

$$F_3 = \frac{1 - \exp[(0.63 \times T_o + 2.68 \times \mathrm{RH} - 0.12 \times \mathrm{WS} + 3.55 \times \mathrm{SR} - 1.09 \times T_F - 0.48 \times M_F + 1.65 \times \mathrm{TDS}_F) - 2.92]}{1 + \exp[(0.63 \times T_o + 2.68 \times \mathrm{RH} - 0.12 \times \mathrm{WS} + 3.55 \times \mathrm{SR} - 1.09 \times T_F - 0.48 \times M_F + 1.65 \times \mathrm{TDS}_F) - 2.92]} \quad (15)$$

$$F_4 = \frac{1 - \exp[(-0.57 \times T_o + 1.07 \times \mathrm{RH} - 1.08 \times \mathrm{WS} - 0.56 \times \mathrm{SR} - 0.62 \times T_F - 0.74 \times M_F - 0.04 \times \mathrm{TDS}_F) + 0.90]}{1 + \exp[(-0.57 \times T_o + 1.07 \times \mathrm{RH} - 1.08 \times \mathrm{WS} - 0.56 \times \mathrm{SR} - 0.62 \times T_F - 0.74 \times M_F - 0.04 \times \mathrm{TDS}_F) + 0.90]} \quad (16)$$

$$F_5 = \frac{1 - \exp[(-0.57 \times T_o - 0.41 \times \mathrm{RH} - 0.46 \times \mathrm{WS} - 0.85 \times \mathrm{SR} + 0.06 \times T_F - 0.23 \times M_F + 0.15 \times \mathrm{TDS}_F) + 0.45]}{1 + \exp[(-0.57 \times T_o - 0.41 \times \mathrm{RH} - 0.46 \times \mathrm{WS} - 0.85 \times \mathrm{SR} + 0.06 \times T_F - 0.23 \times M_F + 0.15 \times \mathrm{TDS}_F) + 0.45]} \quad (17)$$

Table 5
Standard error (SE) of regression coefficients, t statistic (t-stat), and probability (p-value) of MLR model parameters

Model parameters	SE	t-stat	p-value
Intercept	0.635	−0.635	0.530
T_o	0.010	2.767	0.009
RH	0.002	2.813	0.008
WS	0.010	0.280	0.781
SR	0.000	22.028	0.000
T_F	0.013	−1.538	0.134
M_F	2.922	−0.355	0.725
TDS_F	0.001	0.835	0.410

estimate of the coefficient. The smaller the SE, the more accurate the estimate. According to Table 6, the SE of the SR is the smallest. The significance of each coefficient of the obtained MLR model was determined by t-stat and p-value, which are shown in Table 5. The larger the t-stat and the smaller the p-value, the more significant is the corresponding coefficient. The absolute value of the t-stat should be greater than the critical t value. The t-stat values of T_o, RH and SR are greater than 2.040 (critical t value at 31 degrees of freedom) which indicates the accuracy of the coefficients of these variables. Table 5 demonstrates the degrees of meaningfulness of the input parameters of the MLR model. These degrees of meaningfulness are determined by having p-value that is less than the significance level α (0.05). By examining the p-values, it was revealed that there is a significant relationship between independent variables (T_o, RH, and SR) and dependent variable (MD) at a statistical significance level 0.05. While WS, T_F, M_F, and TDS_F were not statistically significant as p-value is greater than 0.05. SR is the most significant variable in the MLR model with the highest t-stat and smallest p-value. The significance ranking of input variables is determined as SR, RH, and T_o.

The comparison of the observed results, ANN prediction results, and MLR prediction results is illustrated in Fig. 4, for the training, testing, and validation

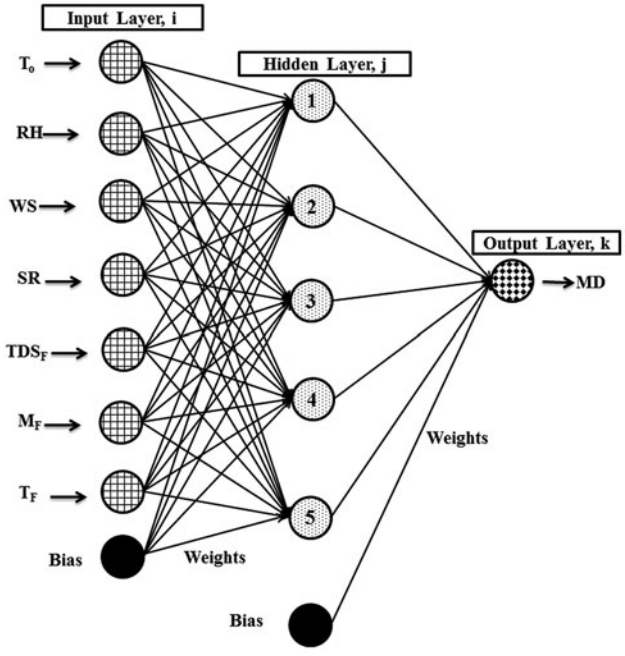

Fig. 3. Optimal architecture of the ANN model used for prediction of the MD.

data sets. The comparison in Fig. 4, reveals that the ANN prediction values are closer to the observed values than are the MLR prediction values. The consistent agreement between the predicted and observed values demonstrates the reliability of the developed ANN model for predicting MD. The overall performance of the ANN and MLR models was assessed using the statistical analyses, as shown in Table 6. Fig. 4 shows that during the training process, the values forecast by the developed ANN model fit perfectly with the observed values. The values predicted using the ANN model were mostly evenly and tightly distributed around the 1:1 line as presented in Fig. 4. Furthermore, the R^2 (0.989) value was very close to one

Table 6
Statistical parameters for assessing the performance of the ANN and MLR models during training, testing, and validation phases

	Training		Testing		Validation	
Statistical parameters	ANN	MLR	ANN	MLR	ANN	MLR
R^2	0.989	0.915	0.917	0.688	0.983	0.941
RMSE	0.018	0.202	0.055	0.212	0.028	0.210
ME	0.989	−0.321	0.913	−0.292	0.981	−0.080
OI	0.982	0.204	0.910	0.176	0.970	0.302
CRM	0.001	−0.321	0.019	−0.299	−0.007	−0.331
MAE	0.015	0.193	0.036	0.187	0.023	0.200

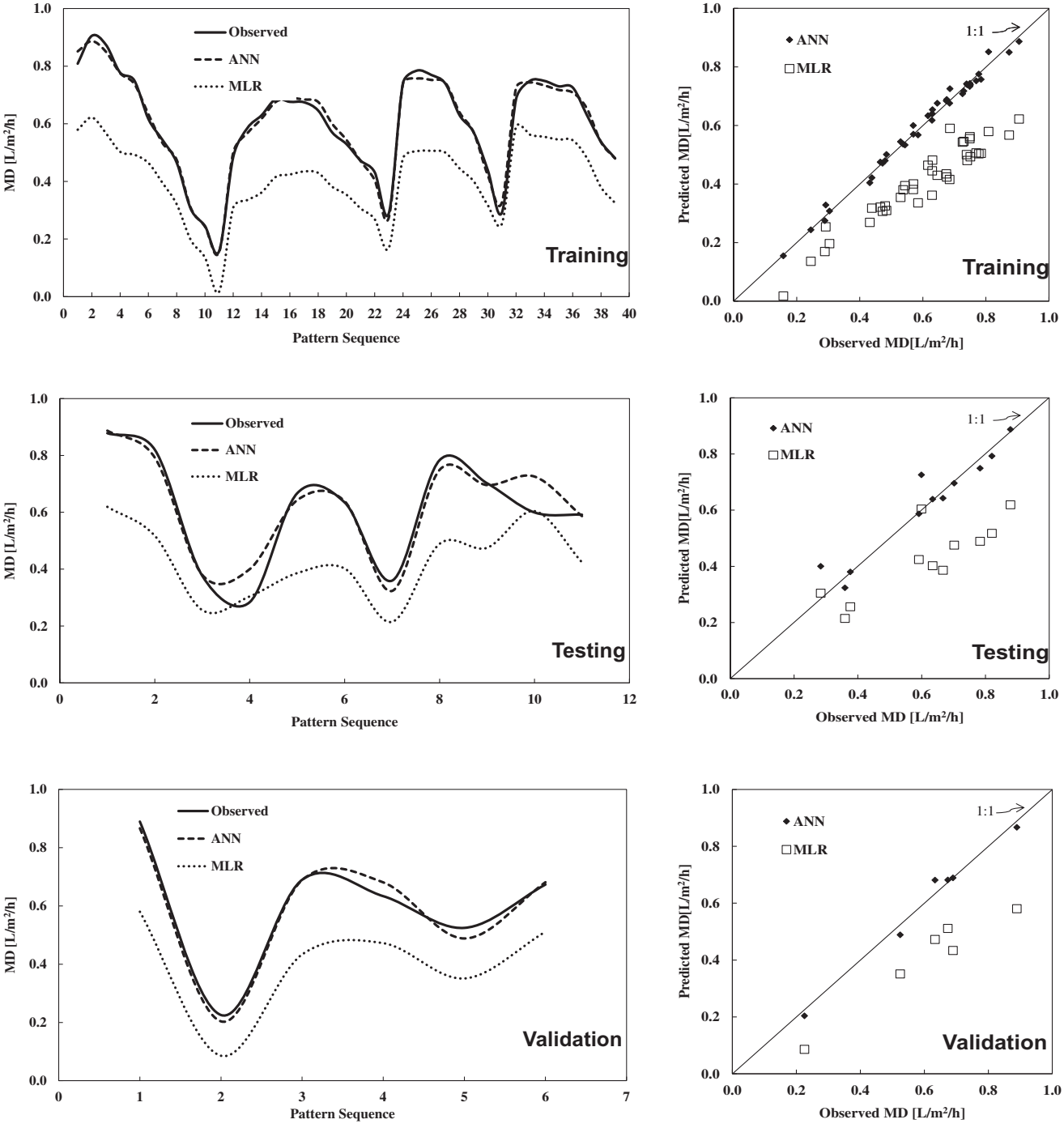

Fig. 4. Comparison between observed and predicted values of MD using ANN and MLR models during the training, testing, and validation stages.

for ANN model. An RMSE value close to zero (specifically, 0.018 $L/m^2/h$) was calculated for the ANN model, as shown in Table 6. The corresponding ME and OI values were 0.989 and 0.982, which are both close to one. The CRM and MAE values were 0.001 and 0.015 $L/m^2/h$, respectively, which are very close to zero. In addition, Fig. 4 reveals that many points obtained for the training stage by using the MLR model are located above and below the 1:1 line. The MLR statistical performance indicators are presented

in Table 6. During the training stage, the MLR model had an R^2 value that was approximately 7.4% less accurate than that of the developed ANN model. The RMSE and MAE values were 11 times and 13 times larger, respectively, than their values in the ANN model. The MLR model reduces the OI value by about 77.8% that of the value for the ANN model and the ME (−0.321) value is very far from one for the MLR model. Fig. 5 depicts the relative errors of the forecasted MD values using ANN and MLR models. During the training process and for ANN model, the relative errors are mostly in the vicinity of ±10%.

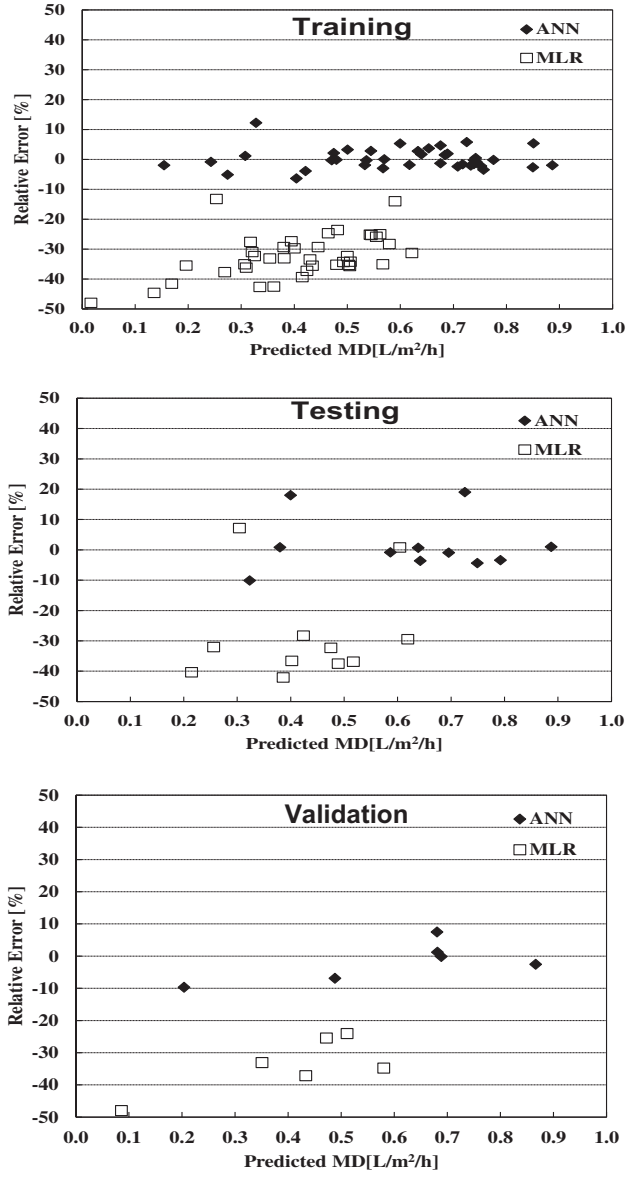

Fig. 5. Relative errors for the ANN model and the MLR model using the training, testing, and validation data-sets.

While, as stated in Fig. 5, the relative errors using the MLR model are more than that from the ANN model which show that the developed ANN model is sufficiently accurate.

Further, Fig. 4 illustrates the relationship between the observed and predicted values of MD using the ANN and MLR models during the testing process. As occurred in the training process, the developed ANN model gave better agreement between the observed and predicted values than the MLR model. As indicated in the figure, the majority of the MD values for the ANN model followed the 1:1 line during the testing process. Thus, showing a very good match between the predicted and observed findings. The statistical parameters R^2, RMSE, ME, OI, CRM, and MAE used to assess the agreement between the observed and predicted values by the ANN and MLR models using the testing data-set are presented in Table 6. The R^2, ME, and OI values were close to one using the developed ANN model during the testing process indicating an excellent agreement between the observed and predicted values using the developed ANN model. In contrast, the MLR model using the testing data-set had R^2, ME, and OI values that were 22.9, 120.5, and 73.4%, respectively, and thus were less accurate than those from the developed ANN model. Moreover, in Table 6 it can be noted that the values of RMSE, CRM, and MAE are low for the MD predicted from the ANN model and high for the MD predicted by the MLR model. The value of RMSE for the MLR model (0.212 L/m^2/h) was about 4 times that of the value for the developed ANN model (0.055 L/m^2/h). The CRM value for the ANN model was closer to zero than its value for the MLR model. Additionally, the CRM value for the MLR model was 15 times that of the value for the developed ANN model. The MAE value of 0.187 L/m^2/h in the MLR model was 419.44% higher than those from the developed ANN model (0.036 L/m^2/h). Plotting of the relative errors during the testing process is presented in Fig. 5. The ANN model in Fig. 5 can be used to predict MD with errors (82% of the values) ranging mostly from −10% to +10%. On the other hand, using the MLR model, the relative error values falling within ±10% represent less than 19% of the whole error values during the testing process.

A comparison of the observed results, the ANN prediction results and the MLR prediction results for the validation data-set is shown in Fig. 4. The figure shows that the MD mostly followed a 1:1 line during the validation process for the developed ANN model, demonstrating a very good match between the predicted and observed data. As occurred in the training and testing processes, the developed ANN model

gave better agreement between the observed and predicted values than the MLR model. The ANN model gave value for R^2 of 0.983. As indicated in Table 6, the RMSE and MAE values were very low, whilst the R^2, ME, and OI values were close to one. Also, the CRM (−0.007) value was very close to zero. On the contrary, the MLR model had an R^2 value that was about 4.2% less accurate than that from the developed ANN model. The value of RMSE for the MLR model (0.210 $L/m^2/h$) was about 8 times that of the value for the ANN model. The MLR model had an ME value that was about 106.1% less accurate than that from the developed ANN model. The OI (0.302) value for the MLR model was far from one. Furthermore, the CRM value for the MLR was about 50 times that of the value for the ANN model. The MAE value of 0.200 for the MLR model was increased by 769.57% than that from the ANN model. The relative error of the predicted MD values for the validation data-set for the ANN model and the MLR model is illustrated in Fig. 5. This figure shows the differences between the findings of the two models with an average relative error of −33.77% for the MLR model when using the validation data-set; this indicates the large amount of underestimation in the predicted MD. The corresponding value for the developed ANN model was lower at −1.8% for the validation data-set, demonstrating the small amount of underestimation in the predicted MD.

Once the graphs indicated in Figs. 4, 5 and Table 6 are examined, it appears that the results predicted using the developed ANN model are very close to the observed values. On the other hand, the results obtained using the MLR model showed a higher deviation from the observed values as compared to the developed ANN model for the training, testing, and validation data-sets. From all of the above, it can be claimed that the developed ANN model is accurately trained and shows consistency in forecasting MD. This result increases the reliability of the developed ANN model. Moreover, it is revealed that the ANN model can forecast MD without needing more experiential work that requires more time and involves high costs. Overall, the comparison between the ANN and MLR models demonstrated that the ANN model can predict MD better than the MLR model on the training set, testing set, and validation set. These results are in conformity with the findings of Safa and Samarasinghe [11], and Mashaly and Alazba [22].

4. Conclusion

Desalination of agricultural drainage water (ADW) may be a strategic choice to deal with the continuing increase in water demand. Implementation of solar still technology for ADW desalination would require an optimization process because of the high capital costs involved with solar distillation, primarily land and equipment. Precise prediction of expected productivity of the solar still is vital to the success of the entire process to optimize expenditures and maximize productivity. This paper presents an ANN model to predict the water productivity (MD) of solar still desalinating ADW. The ANN model was developed based on a feed-forward back-propagation algorithm. Its feasibility for MD prediction was checked. Many neural network configurations with different numbers of neurons in the hidden layer were trained to determine which architecture gave the optimal performance.

Seven input variables were inputs to the ANN model in the input layer, namely air temperature (T_o), relative humidity (RH), wind speed (WS), solar radiation (SR), temperature of feedwater (T_F), total dissolved solids of feedwater (TDS_F), and flow rate of feedwater (M_F). One neuron in the output layer that represented the output (MD). The optimal ANN architecture was selected by a trial-and-error method. Five neurons were the best number of neurons in the hidden layer. The 7–5–1 architecture was the optimal ANN architecture. The hyperbolic tangent (TANH) function was the best transfer function in the hidden and output layers. The findings were compared with those from MLR. The performance of the models was evaluated by the statistical parameters, R^2, RMSE, ME, OI, CRM, and MAE, which are numerical indicators used to assess the agreement between observed and predicted MD. In all stages of the modeling process, namely training, testing, and validation stages, the developed ANN model showed performance higher than MLR. The statistical parameter values support the strength and applicability of the developed ANN prediction model. The results also confirmed the accuracy and generalization ability of the ANN model. The study demonstrates that the ANN model can be used as a design tool to predict the MD of solar still for ADW desalination and adds value to the optimization process by decreasing time and engineering effort spent in experiments. Finally, the prediction of MD will facilitate the development of plans to benefit from the desalinated ADW either directly or indirectly through mixing with water of low quality to increase the volume of water available for agricultural sectors. This will help in achieving global water and food security.

Acknowledgment

The project was financially supported by King Saud University, Vice Deanship of Research Chairs.

List of symbols

ADW	—	agricultural drainage water
ANN	—	artificial neural network
BP	—	back propagation
CC	—	correlation coefficient
CRM	—	coefficient of residual mass
MAE	—	mean absolute error
MD	—	solar still productivity
ME	—	coefficient of model efficiency
M_F	—	feed flow rate
MLP	—	multilayer perceptron
MLR	—	multiple linear regression
MXE	—	maximum error
OI	—	overall index of model performance
R^2	—	coefficient of determination
RH	—	relative humidity
RMSE	—	root mean square error
SD	—	standard deviation
SIG	—	sigmoid transfer function
SR	—	solar radiation
TANH	—	hyperbolic tangent transfer function
TDS_F	—	total dissolved solids of feedwater
T_F	—	temperature of feedwater
T_o	—	ambient temperature
WS	—	wind speed

References

[1] M.H. Sorour, N.M.H. El Defrawy, H.F. Shaalan, Treatment of agricultural drainage water via lagoon/reverse osmosis system, Desalination 152 (2003) 359–366.

[2] P.J. Gregory, Soils and food security: Challenges and opportunities, in: R.E. Hester, R.M. Harrison (Eds.), Soils and Food Security, RSC Publishing, London, 2012, pp. 1–30.

[3] A. Rahardianto, B.C. McCool, Y. Cohen, Reverse osmosis desalting of inland brackish water of high gypsum scaling propensity: Kinetics and mitigation of membrane mineral scaling, Environ. Sci. Technol. 42 (2008) 4292–4297.

[4] D. Zarzo, E. Campos, P. Terrero, Spanish experience in desalination for agriculture, Desalin. Water Treat. 51 (2013) 53–66.

[5] S. Burn, M. Hoang, D. Zarzo, F. Olewniak, E. Campos, B. Bolto, O. Barron, Desalination techniques—A review of the opportunities for desalination in agriculture, Desalination 364 (2015) 2–16.

[6] G.M. Ayoub, L. Malaeb, Developments in solar still desalination systems: A critical review, Crit. Rev. Environ. Sci. Technol. 42 (2012) 2078–2112.

[7] R.S. Adhikari, A. Kumar, M.S. Sodha, Thermal performance of a multi-effect diffusion solar still, Int. J. Energy Res. 15 (1991) 769–779.

[8] M. Hamdan, R.H. Khalil, E. Abdelhafez, Comparison of neural network models in the estimation of the performance of solar still under Jordanian climate, J. Clean Energy Technol. 1 (2013) 238–242.

[9] Y.A. Pachepsky, D. Timlin, G. Varallyay, Artificial neural networks to estimate soil water retention from easily measurable data, Soil Sci. Soc. Am. J. 60 (1996) 727–733.

[10] D. Elizondo, G. Hoogenboom, R.W. Mcclendon, Development of a neural network model to predict daily solar radiation, Agric. For. Meteorol. 71 (1994) 115–132.

[11] M. Safa, S. Samarasinghe, Determination and modelling of energy consumption in wheat production using neural networks: A case study in Canterbury province, New Zealand, Energy 36 (2011) 5140–5147.

[12] M. Gocić, S. Motamedi, S. Shamshirband, D. Petković, S. Ch, R. Hashim, M. Arif, Soft computing approaches for forecasting reference evapotranspiration, Comput. Electron. Agric. 113 (2015) 164–173.

[13] C.C. Yang, S.O. Prasher, R. Lacroix, Applications of artificial neural networks to land drainage engineering, Trans. ASAE 39 (1996) 525–533.

[14] S.M. KAshefipour, M.K. Sadr, A.A. Naseri Modelling drainage water salinity for agricultural lands under leaching using artificial neural networks, Sol. Energy 61 (2012) 99–106.

[15] M. Schaap, W. Bouten, Modeling water retention curves of sandy soils using neural networks, Water Resour. Res. 32 (1996) 3033–3040.

[16] S. Lecoeuche, S. Lalot, Prediction of the daily performance of solar collectors, Int. Commun. Heat Mass Transfer 32 (2005) 603–611.

[17] I. Farkas, P. Géczy-Víg, Neural network modelling of flat-plate solar collectors, Comput. Electron. Agric. 40 (2003) 87–102.

[18] A. Sözen, T. Menlik, S. Ünvar, Determination of efficiency of flat-plate solar collectors using neural network approach, Expert Syst. Applic. 35 (2008) 1533–1539.

[19] N.I. Santos, A.M. Said, D.E. James, N.H. Venkatesh, Modeling solar still production using local weather data and artificial neural networks, Renewable Energy 40 (2012) 71–79.

[20] A.F. Mashaly, A.A. Alazba, Comparative investigation of artificial neural network learning algorithms for modeling solar still production, J. Water Reuse Desalin. 5(4) (2015) 480–493.

[21] A.F. Mashaly, A.A. Alazba, A.M. Al-Awaadh, M.A. Mattar, Predictive model for assessing and optimizing solar still performance using artificial neural network under hyper arid environment, Solar Energy 118 (2015) 41–58.

[22] A.F. Mashaly, A.A. Alazba, MLP and MLR models for instantaneous thermal efficiency prediction of solar still under hyper-arid environment, J. Energy Inst. 122 (2016) 146–155.

[23] S. Haykin, Neural Networks: A Comprehensive Foundation, second ed., Prentice Hall, New Jersey, NJ, 1999.

[24] S. Kalogirou, S. Panteliou, A. Dentsoras, Artificial neural networks used for the performance prediction of a thermosiphon solar water heater, Renewable Energy 18 (1999) 87–99.

[25] H. Kurt, K. Atik, M. Ozkaymak, A.K. Binark, Artificial neural network approach for evaluation of temperature and density profiles of salt gradient solar pond, J. Energy Inst. 80 (2007) 46–51.

[26] R. Pahlavan, M. Omid, A. Akram, Energy input–output analysis and application of artificial neural

networks for predicting greenhouse basil production, Energy 37 (2012) 171–176.
[27] H. Demuth, M. Beale, Neural Network Toolbox: For Use with MATLAB (Version 4.0), The MathWorks, Inc., Natick, MA, 2004.
[28] A.M. Hassan, A. Alrashdan, M.T. Hayajneh, A.T. Mayyas, Prediction of density, porosity and hardness in aluminum-copper-based composite materials using artificial neural network, J. Mater. Process. Technol. 209 (2009) 894–899.
[29] C. Buratti, L. Barelli, E. Moretti, Wooden windows: Sound insulation evaluation by means of artificial neural networks, Appl. Acoust. 74 (2013) 740–745.
[30] D.E. Rumelhart, G.E. Hinton, R.J. Williams, Learning Internal Representations by Error Propagation. In: Parallel Distributed Processing: Explorations in the Microstructure of Cognition, vol. 1, Chapter 8, MIT Press, Cambridge, MA, 1986.
[31] A.S. Abutaleb, A neural network for the estimation of forces acting on radar targets, Neural Netw. 4 (1991) 667–678.
[32] R. Scheaffer, M. Mulekar, J. McClav, Probability and Statistics for Engineers, fifth ed., Brooks/Cole, Boston, 2011, p. 599.
[33] M.M. Rahman, B.K. Bala, Modelling of jute production using artificial neural networks, Biosyst. Eng. 105 (2010) 350–356.
[34] M. Zangeneh, M. Omid, A. Akram, A comparative study between parametric and artificial neural networks approaches for economical assessment of potato production in Iran, Spanish J. Agric. Res. 9 (2011) 661–671.
[35] A.A. Alazba, M.A. Mattar, M.N. ElNesr, M.T. Amin, Field assessment of friction head loss and friction correction factor equations, J. Irrig. Drain. Eng. 138 (2012) 166–176.
[36] A.F. Mashaly, A.A. Alazba, A.M. Al-Awaadh, Assessing the performance of solar desalination system to approach near-ZLD under hyper arid environment, Desalin. Water Treat. 57 (2016) 12019–12036.
[37] WHO, Guidelines for Drinking-Water Quality, third ed., World Health Organization, Geneva, 2004.
[38] H.E.S. Fath, S.M. El-Sherbiny, A. Ghazy, Transient analysis of a new humidification–dehumidification solar still, Desalination 155 (2003) 187–203.
[39] A.M. Radhwan, Transient performance of a steeped solar still with built-in latent heat thermal energy storage, Desalination 171 (2004) 61–71.
[40] S.B. Sadineni, R. Hurt, C.K. Halford, R.F. Boehm, Theory and experimental investigation of a weir type inclined solar still, Energy 33 (2008) 71–80.
[41] A.E. Kabeel, E.A. Elkenany, O.M. Hawam, Experimental study of the performance of solar still using a reciprocating intermittent spray feeding system, J. Renewable Sustainable Energy 5 (2013) 013108.
[42] A. Muthu Manokar, K. Kalidasa Murugavel, G. Esakkimuthu, Different parameters affecting the rate of evaporation and condensation on passive solar still—A review, Desalination 38 (2014) 309–322.
[43] A.F. Mashaly, A.A. Alazba, A.M. Al-Awaadh, M.A. Mattar, Area determination of solar desalination system for irrigating crops in greenhouses using different quality feed water, Agric. Water Manage. 154 (2015) 1–10.
[44] M.A. Antar, S.M. Zubair, Performance evaluation of a solar still in the Eastern Province of Saudi Arabia—An improved analysis, Desalin. Water Treat. 22 (2010) 100–110.
[45] V. Velmurugan, J. Mandlin, B. Stalin, K. Srithar, Augmentation of saline streams in solar stills integrating with a mini solar pond, Desalination 249 (2009) 143–149.